Characteristics of n-type ZnO nanorods on top of p-type poly(3-hexylthiophene) heterojunction by solution-based growth

Chun-Yu Lee [a], Jing-Shun Huang [a], Sheng-Hao Hsu [b], Wei-Fang Su [c,d], Ching-Fuh Lin [a,e,f,]*

[a] Graduate Institute of Photonics and Optoelectronics, National Taiwan University, Taipei 10617, Taiwan
[b] Institute of Polymer Science and Engineering, National Taiwan University, Taipei 10617, Taiwan
[c] Graduate Institute of Materials Science and Engineering, National Taiwan University, Taipei 10617, Taiwan
[d] Department of Materials Science and Engineering, National Taiwan University, Taipei 10617, Taiwan
[e] Graduate Institute of Electronics Engineering, National Taiwan University, Taipei 10617, Taiwan
[f] Department of Electrical Engineering, National Taiwan University, Taipei 10617, Taiwan

ARTICLE INFO

ABSTRACT

We report that ZnO nanorods (NRs) are grown on an organic layer of poly(3-hexylthiophene) (P3HT) using a modified seeding layer. Thus, ZnO NRs/P3HT heterojunction light-emitting diodes could be fabricated using the hydrothermal method, in which ZnO acts as an n-type material and P3HT as a p-type material. The ZnO NRs improve the electron transportation in the devices. A three-fold enhancement of current density of the device is observed due to the NRs formed on the P3HT. The electroluminescence (EL) of the optimized ZnO-based device is 1.5 times larger than that without NRs. The influence of the P3HT thickness for the EL spectrum is also discussed.

1. Introduction

Organic light-emitting diodes (OLEDs) have been widely studied for their potential applications in full-color-flat-panel displays and large area light-emitting devices (LED) [1,2]. To realize practical LED applications, it is necessary to fabricate a p–n junction [3,4]. However, the mobility of electrons in most organic material is much lower than that of holes, which causes imbalanced carrier injection in organic electroluminescent devices [5]. On the other hand, inorganic semiconductors such as ZnO have higher electron mobility [6,7]. Hence, the ZnO/organic heterostructure provides an approach for the balance of the hole and electron current densities to construct high-performance electroluminescence (EL) devices [8–10].

ZnO has been widely fabricated on inorganic substrates, such as GaN [11], NiO [12], silicon wafer [13], and sapphire [14], to form the p–n heterostructure. In contrast, the formation of ZnO on organic materials has remained a challenge. Recently, ZnO thin film on poly[2-methoxy-5-(2-ethylhexyloxy)-1,4-phenylenevinylene] (MEHPPV)

have been produced by electron beam evaporation [15]. The above work involves the vacuum deposition of ZnO, which is usually inconvenient and expensive. Here, we present a straightforward and versatile, solution-based method to grow the n-type inorganic material of a ZnO nanorod (NR) array on a p-type polymer to fabricate the p–n junction diodes. We demonstrate that the ZnO NR array leads to a significant improvement of the electrical properties of the OLED.

In this work, a ZnO NR array is fabricated using a hydrothermal method on a p-type conducting polymer of poly(3-hexylthiophene) (P3HT) thin film at low temperature (90 °C). The P3HT layer is deposited using the spin-coating method. The electrical characteristics of a ZnO-based inorganic–organic p–n junction are investigated. The ZnO-based p–n junction shows very good rectifying behavior. The strong visible EL is obtained from the junction at room temperature. The results reported here suggest that a ZnO-based p–n junction diode can be realized using this comparatively easy method.

2. Experimental details

The schematic illustrations of the ZnO-based p–n junction structure are shown in Fig. 1. The fabrication started from the

* Corresponding author. BL building 414, No. 1, Sec. 4, Roosevelt Road, Taipei, 10617 Taiwan. Tel.: +886 2 3366 3540; fax: +886 2 2364 2603.
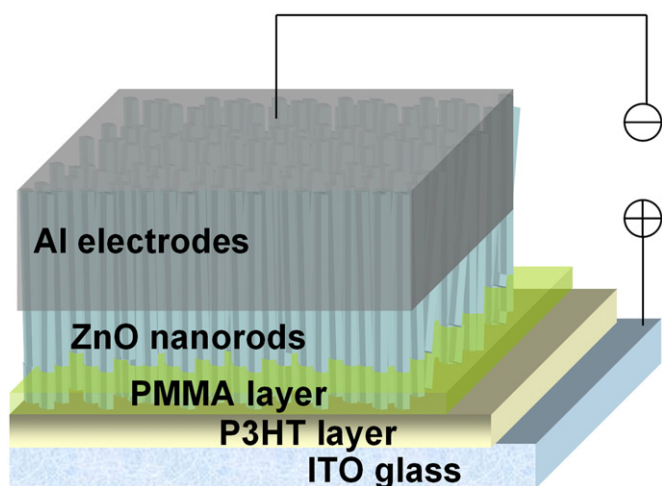E-mail address: cflin@cc.ee.ntu.edu.tw (C.-F. Lin).

Fig. 1. Schematic illustration of the ZnO NRs/P3HT thin film heterojunction LED.

preparation of P3HT thin film on indium tin oxide (ITO)-coated glass by spin coating P3HT from solution in chloroform with a spin rate of 4000 rpm for 80 s. The solution was formed by dissolving the polymer powder in chloroform with a concentration of 0.7 wt.% at around 50 °C for 1 h. The sample was subsequently annealed at 120 °C for 2 h to remove the solvent. To facilitate the nucleation of ZnO NR growth, a seeding layer was formed on top of the P3HT thin film by spin coating with a ZnO seeding solution. The concentration of the ZnO seeding solution was chosen to be 0.5 M. Afterwards, the seeding layer was annealed at 100 °C for 1 h to remove the residual solvent. Then, we employed a hydrothermal method to grow ZnO NRs on top of the P3HT layer. The hydrothermal growth of the ZnO NR array was achieved by suspending the seeding layer-coated P3HT layer upside down in an aqueous solution of 50 mM zinc nitrate hexahydrate [Zn(NO3)2·6H2O, Sigma Aldrich, 98% purity] and 50 mM hexamethylenetetramine [C6H12N4,Sigma Aldrich, 99.5% purity] at a low temperature of 90 °C for 3 h [16]. At the end of the growth period, the sample was washed repeatedly with deionized water and dried in air for characterization. Poly(methyl methacrylate) (PMMA) dissolved in chloroform with a concentration of 0.5 wt.% was spin-coated on the hydrothermally grown product with a spin rate of 4000 rpm for 80 s to electrically isolate the ZnO NRs. Oxygen plasma etching (200 W for 20 s) was then used to remove the PMMA coated on top of the ZnO NRs to expose them for metallization [17,18]. Finally, an aluminum (Al) electrode was deposited by thermal evaporation (ULVAC, VPC-410) in a high vacuum condition of about 2×10^{-6} Torr to provide a contact for electron injection. The defined emitting area was 3×5 mm.

It is not easy to produce an n-type ZnO array on p-type conducting polymers because it is difficult to form a good film on top of the conducting polymer during spin coating with the general seeding solution containing zinc acetate dehydrate, monoethanolamine, and 2-methoxyethanol [19]. The seeding solution is hydrophilic and most of the conducting polymer films such as P3HT, MEHPPV, poly(3-octylthiophene), poly(N-vinylcarbazole), poly[2-methoxy-5-(3′,7′-dimethyloctyloxy)-1,4-phenylenevinylene], and poly(fluorine) are hydrophobic. In order to deposit the seeding layer on the conducting polymer well, we added glycerol into the seeding solution in the proper proportion. The modified seeding solution was then stirred at 120 °C for 1 h to yield a homogeneous and stable colloid solution, which served as the coating solution. We found that glycerol is one of the few solvents that is compatible and innoxious to the conducting polymer. The addition of glycerol results in a decrease in the hydrophilicity of the seeding solution. The heated seeding solution improves the film-forming property of the seeding layer on the P3HT

by decreasing the surface tension of the seeding layer as the temperature increases during spin coating.

3. Results and discussion

Field emission scanning electron microscopy (FESEM, LEO-1530, LEO, Oberkochen, Germany) was utilized to examine the formation of the ZnO NR array on the P3HT. The operating voltage of the FESEM electron gun was 5 kV. With the modified deposition of the seeding layer on the P3HT, the growth of the ZnO NR array consists of compact, closely packed NRs, as shown in Fig. 2a. The average diameter of the ZnO NR that formed on the surface of the P3HT was about 330 ± 50 nm. For the cross-sectional view in Fig. 2b, the average length of the ZnO NR and the thickness of the P3HT on the ITO-coated glass were about 2.8 μm and 240 nm, respectively. In contrast, we grew the NRs on the P3HT without improving the deposition condition of the seeding layer. The density and size of the NRs had striking changes, as seen in the inset of Fig. 2a. Hence, the density and size of the ZnO NRs strongly depend on the modified seeding layer. Fig. 2c and d shows that a very thin PMMA coating on top of the NRs can be achieved, while the space between the NRs is solidly filled with the PMMA. As illustrated in Fig. 2c, an insulator layer of the PMMA deposition and a filling of the spaces between the ZnO NRs were found. Fig. 2d reveals that a PMMA coating on top of the ZnO NRs can be achieved. According to the spin-coating parameter and electron micrograph, we estimate the PMMA thickness on the ZnO NR tips to be in the range of 30–50 nm. The thickness is comparable to the thickness obtained on planar ITO glass using similar experimental conditions, i.e., concentration, molecular weight, spin rate, etc., as used here. Fig. 2e and f exhibits the change of the ZnO NRs:PMMA on the P3HT after oxygen plasma etching. Obviously, only the tips of the ZnO NRs were exposed, while the roots were still covered with PMMA. Furthermore, the mean diameter of the ZnO NRs decreased from 330 nm to 280 nm. We believe that the diameters of the ZnO NRs probably were reduced due to the etching effect of high-power plasma (200 W for 20 s) [20,21]. The residues of PMMA left near the roots of the ZnO NRs after oxygen plasma etching can be explained by the short etching time (20 s). Fig. 2g and h shows the top view and cross-sectional FESEM images of the final structure of the ZnO NRs/P3HT heterojunction diode. It can be seen that the ZnO NRs:PMMA/P3HT nanostructure is covered with a continuous Al coating. Though the surface is still rough after Al deposition, the tips of the ZnO NRs can be covered well by the Al coating.

The crystallinity of the ZnO NRs on the P3HT was examined at room temperature using a Nonious CAD4 Kappa Axis XRD instrument with CuKα radiation operating at 40 kV and 25 mA, and a scan rate of 3°/min. The CAD4 was equipped with a scintillation detector, a liquid-nitrogen low-temperature device, and a long 2theta-detector arm on a Nonius FR571 X-ray generator with a copper rotating anode. X-rays were produced by the source at 1.5418 Å. XRD analysis shows that as-grown ZnO NRs have a wurtzite structure. In Fig. 3, several diffraction peaks can be observed at $2\theta = 31.74°$, 34.44°, 36.26°, 47.48°, 56.66°, and 62.93°, which is due to ZnO (100), (002), (101), (102), (110), and (103), respectively. The diffraction peaks agree with the JCPDS card No. 36-1451, corresponding to the hexagonal wurtzite structure of ZnO.

The current–voltage characteristics were measured using a source meter (Model-2400, Keithley, USA) under ambient air at room temperature conditions and without encapsulation. Three kinds of devices were fabricated for comparison: ITO/P3HT (240 nm)/Al (device A); ITO/P3HT (240 nm)/ZnO NRs:PMMA/Al (device B); and ITO/P3HT (~300 nm)/ZnO NRs:PMMA/Al (device C). The current–voltage characteristics in the DC bias mode of device A (without ZnO NRs), B, and C (with ZnO NRs) are shown in Fig. 4. It was observed that the heterojunction diodes (devices B and C) clearly demonstrate a desirable rectifying behavior of the p–n junction, and the single-layer
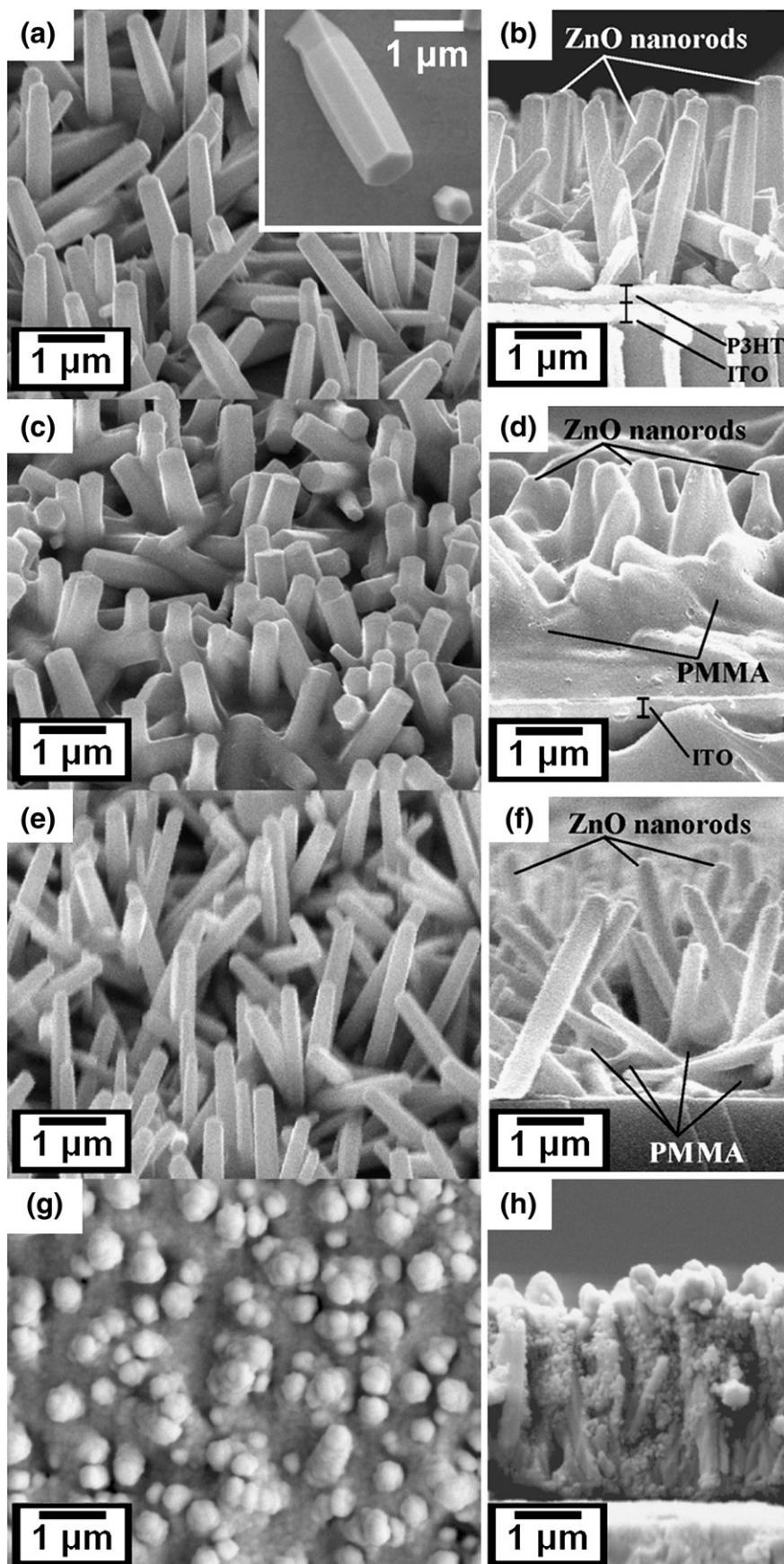
Fig. 2. FESEM images of the tilted view (45°) and cross-section view of (a and b) ZnO NRs grown on P3HT thin film, (c and d) after deposit of PMMA, and (e and f) after PMMA etching to expose the NR tips. FESEM images of top and cross-section views of (g and h) the final structure of Al contact on the ZnO NRs embedded in the PMMA. The inset image shows the growth of ZnO NRs on the P3HT with an unmodified seeding layer.
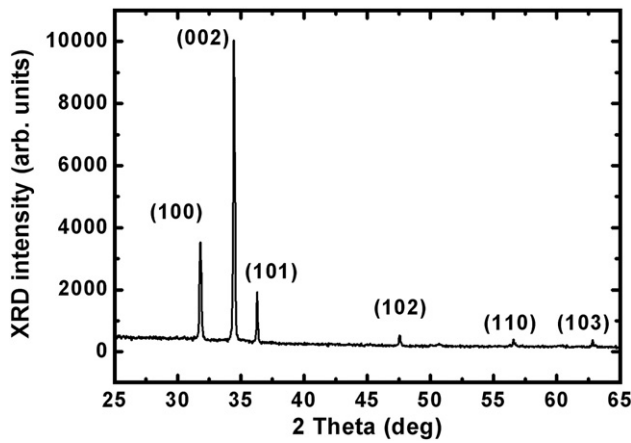
Fig. 3. XRD pattern of ZnO NRs on the P3HT prepared with a hydrothermal method at 90 °C using zinc nitrate as the zinc source.

Fig. 5. The room temperature EL spectra for a forward DC bias of 10 V for (a) ITO/P3HT (240 nm)/Al; (b) ITO/P3HT (240 nm)/ZnO NRs:PMMA/Al; and (c) ITO/P3HT (300 nm)/ZnO NRs:PMMA/Al.

structure of device A also shows a stable rectifying behavior. The rectifying behavior of device A can be understood by examining the energy level diagram of device A [22]. At the P3HT/electrode interface, the potential barriers of both electrons and holes under reverse bias are much higher than those of forward bias. That is to say, carriers cannot easily be injected from the electrode into the P3HT under reverse bias, but a large number of carriers can be injected from the electrode into the P3HT under forward bias. This is the reason that the single-layer structure of device A exhibits rectifying characteristics. In addition, the device with the ZnO NR array showed a three-fold enhancement of current density at the same voltage and relatively lower driving voltage of 2 V than the device without an ZnO NR array (device A). We attribute this phenomenon to two main reasons. First, the carrier mobility of the ZnO NRs array/P3HT heterostructure is higher than that of the P3HT film only [23,24]. Second, the injection current of the ZnO NRs array/P3HT heterostructure is larger than that of the P3HT film only. The injection current can be enhanced because of the increased carrier injection rate through nanosized contacts at the junction interface between the ZnO NRs and a P3HT layer, similar to what has been indicated in previous reports [3,25,26].

The EL spectra of the devices with a forward DC bias of 10 V are shown in Fig. 5. The EL spectra were characterized using a photomultiplier tube (R928, HAMAMATSU, Japan) attached to a monochromator (model CM110, CVI Laser Spectral Products, USA) under ambient air at room temperature. Light emission from the sample passes through an aperture, a light chopper, and finally

through the entrance slit of a CM110, where the intensity can be resolved at very narrow wavelength intervals. The intensity is detected with an R928 and a lock-in amplifier (SR830, Stanford Research System, USA). For the ZnO-based device, a strong P3HT-relatived emission can be seen (device B). In comparison with the device without a ZnO NR array (device A), the emission intensity increased ~1.5 times and the spectrum peak shifted slightly from 670 nm to 652 nm. We speculate that the growth of the ZnO NR array on top of a P3HT layer induces a change in the local electronic structure of the surface of the P3HT [27,28] due to the interaction between the P3HT molecules and the hydroxyl groups of the ZnO NR surface. This leads to a blue-shifted and broadening EL spectrum while carriers recombine in the interface between the ZnO NR array and the P3HT. In addition, it is clear that the ZnO NRs enhance carrier injection to increase the probability of electron-hole recombination in the EL device. In order to clarify the change in the EL spectrum, we further increased the thickness of the P3HT to ~300 nm. The ZnO-based device with a P3HT thickness of 300 nm (device C) demonstrates an EL emission peak at 670 nm, totally corresponding to the P3HT emission without any shift. This is due to the fact that the mobility of electrons in the ZnO NRs is higher than that of the holes in the P3HT. When the thickness of the P3HT is increased, the recombination zone of the electrons and holes is primarily restricted to the P3HT which is far from the ZnO NRs/P3HT interface. Hence, the EL spectrum of device C is similar to the EL emission from device A. Furthermore, the corresponding I–V curve reveals relatively lower current density than the ZnO-based device with a P3HT thickness of 240 nm due to the thicker conducting polymer [29], as shown in Fig. 4 (device C). The above results account for two phenomena: (1) the location of the carrier recombination between the ZnO NRs/P3HT interface and the P3HT layer strongly depends on the thickness of the P3HT, and (2) the ZnO NRs cause blue-shifted emissions when carrier recombination occurs in the ZnO NRs/P3HT interface.

4. Conclusions

In conclusion, we fabricated ZnO NRs/P3HT heterojunction LEDs, using a p-type polymer (P3HT) and n-type ZnO NRs in all solution process. To optimize the growth of the ZnO NRs on the P3HT, we improved the seeding solution by incorporating glycerol. The EL intensity of the device with the ZnO NRs increased 1.5 times compared to that of the device without ZnO NRs. The ZnO-based device showed a bright EL emission peak at 652 nm under a forward bias of 10 V at room temperature and exhibited a very good rectification characteristic with very low driving voltage of 2 V. The
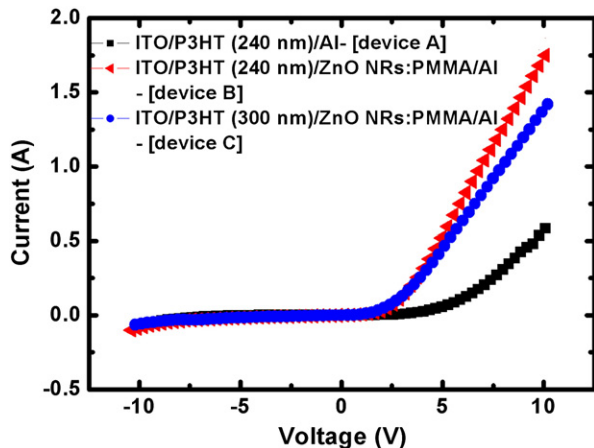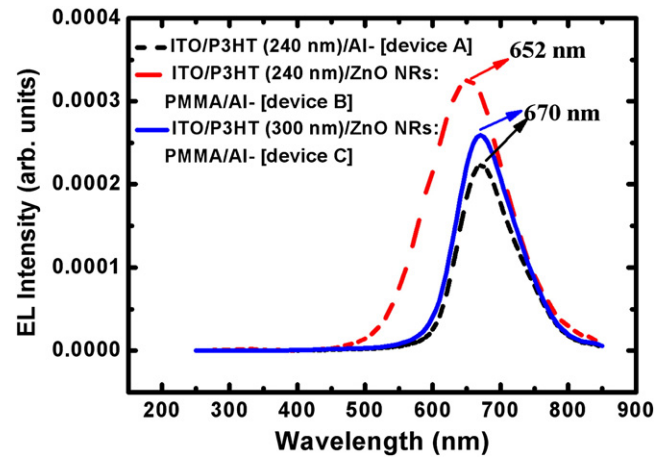

Fig. 4. The room temperature I–V curves in the DC bias mode for (a) ITO/P3HT (240 nm)/Al; (b) ITO/P3HT (240 nm)/ZnO NRs:PMMA/Al; and (c) ITO/P3HT (300 nm)/ZnO NRs:PMMA/Al.

el spectrum depends greatly on the location of the carrier recombination between the ZnO NRS/P3HT interface and the P3HT layer. the ZnO NR array on the P3HT heterojunction diode introduced in this study demonstrates its application potential for LEDs.

References

[1] H.J. Bolink, E. Coronado, D. Repetto, M. Sessolo, Appl. Phys. Lett. 91 (2007) 223501.
[2] H.A. Al Attar, A.P. Monkman, M. Tavasli, S. Bettington, M.R. Bryce, Appl. Phys. Lett. 86 (2005) 121101.
[3] M.C. Jeong, B.Y. Oh, M.H. Ham, J.M. Myoung, Appl. Phys. Lett. 88 (2006) 202105.
[4] J.C. Sun, J.Z. Zhao, H.W. Liang, J.M. Bian, L.Z. Hu, H.Q. Zhang, X.P. Liang, W.F. Liu, G.T. Du, Appl. Phys. Lett. 90 (2007) 121128.
[5] R.W. Chuang, R.X. Wu, L.W. Lai, C.T. Lee, Appl. Phys. Lett. 91 (2007) 231113.
[6] Z.P. Wei, Y.M. Lu, D.Z. Shen, Z.Z. Zhang, B. Yao, B.H. Li, J.Y. Zhang, D.X. Zhao, X.W. Fan, Z.K. Tang, Appl. Phys. Lett. 90 (2007) 042113.
[7] Z.Z. Ye, J.G. Lu, Y.Z. Zhang, Y.J. Zeng, L.L. Chen, F. Zhuge, G.D. Yuan, H.P. He, L.P. Zhu, J.Y. Huang, B.H. Zhao, Appl. Phys. Lett. 91 (2007) 113503.
[8] C.Y. Lee, Y.T. Huang, W.F. Su, C.F. Lin, Appl. Phys. Lett. 89 (2006) 231116.
[9] C.Y. Lee, Y.Y. Hui, W.F. Su, C.F. Lin, Appl. Phys. Lett. 92 (2008) 261107.
[10] M. Nakano, A. Tsukazaki, R.Y. Gunji, K. Ueno, A. Ohtomo, T. Fukumura, M. Kawasaki, Appl. Phys. Lett. 91 (2007) 142113.
[11] S. Mridha, D. Basak, Appl. Phys. Lett. 92 (2008) 142111.
[12] Y.Y. Xi, Y.F. Hsu, A.B. Djurišić, A.M.C. Ng, W.K. Chan, H.L. Tam, K.W. Cheah, Appl. Phys. Lett. 92 (2008) 113505.
[13] L. Duan, B. Lin, W. Zhang, S. Zhong, Z. Fu, Appl. Phys. Lett. 88 (2006) 232110.
[14] H.S. Kim, F. Lugo, S.J. Pearton, D.P. Norton, Y.L. Wang, F. Ren, Appl. Phys. Lett. 92 (2008) 112108.
[15] J. Huang, Z. Xu, S. Zhao, Y. Li, F. Zhang, L. Song, Y. Wang, X. Xu, Solid State Commun. 142 (2007) 417.
[16] Y.R. Lin, S.S. Yang, S.Y. Tsai, H.C. Hsu, S.T. Wu, I.C. Chen, Cryst. Growth Des. 6 (2006) 1951.
[17] X.W. Sun, J.Z. Huang, J.X. Wang, Z. Xu, Nano Lett. 8 (2008) 1219.
[18] T.M. Long, S. Prakash, M.A. Shannon, J.S. Moore, Langmuir 22 (2006) 4104.
[19] M. Afzaal, M.A. Malik, P. O'Brien, New J. Chem. 31 (2007) 2029.
[20] J.H. Park, C.B. Lee, I.S. Kim, S.J. Jang, B.T. Lee, Thin Solid Films 517 (2009) 4432.
[21] T. Sekiguchi, K. Haga, K. Inaba, J. Cryst. Growth 214/215 (2000) 68.
[22] Y.C. Chao, H.F. Meng, S.F. Horng, C.S. Hsu, Org. Electron. 9 (2008) 310.
[23] E. Katsia, N. Huby, G. Tallarida, B. Kutrzeba-Kotowska, M. Perego, S. Ferrari, F.C. Krebs, E. Guziewicz, M. Godlewski, V. Osinniy, G. Luka, Appl. Phys. Lett. 94 (2009) 143501.
[24] C.H. Chen, I. Shih, J. Mater. Sci.: Mater. Electron. 17 (2006) 1047.
[25] S.J. An, G.C. Yi, Appl. Phys. Lett. 91 (2007) 123109.
[26] R. Guo, J. Nishimura, M. Matsumoto, M. Higashihata, D. Nakamura, T. Okada, Appl. Phys. B 94 (2009) 33.
[27] J.P. Richters, T. Voss, L. Wischmeier, I. Rückmann, J. Gutowski, Appl. Phys. Lett. 92 (2008) 011103.
[28] E. Tang, G. Cheng, X. Ma, Powder Technol. 161 (2006) 209.
[29] N.I. Craciun, J.J. Brondijk, P.W.M. Blom, Phys. Rev. B 77 (2008) 035206.